

Thermal-conductivity measurements of GaAs/AlAs superlattices using a picosecond optical pump-and-probe technique

W. S. Capinski and H. J. Maris

Department of Physics, Brown University, Providence, Rhode Island 02912

T. Ruf and M. Cardona

Max-Planck-Institut für Festkörperforschung, Heisenbergstrasse 1, D-70569 Stuttgart, Germany

K. Ploog

Paul-Drude-Institut für Festkörperelektronik, Hausvogteiplatz 5-7, D-10117 Berlin, Germany

D. S. Katzer

Naval Research Laboratory, Washington, D.C. 20375

(Received 17 September 1998)

We present measurements of the lattice thermal conductivity κ_{\perp} normal to the interfaces of $(\text{GaAs})_n/(\text{AlAs})_n$ superlattices with n between 1 and 40 monolayers. The conductivity was measured by an optical pump-and-probe technique in the temperature range of 100 to 375 K. In the experiment, an Al film is deposited onto a superlattice sample, and the rate at which this film cools by conduction into the superlattice is determined. We find a general decrease in κ_{\perp} with a reduction of the superlattice period. At 300 K, κ_{\perp} of the $(\text{GaAs})_{40}/(\text{AlAs})_{40}$ superlattice is approximately three times less than κ of bulk GaAs, and κ_{\perp} of the $(\text{GaAs})_1/(\text{AlAs})_1$ superlattice is an order of magnitude less than κ of bulk GaAs. We discuss the decrease in κ_{\perp} compared to the bulk constituents in terms of extrinsic and intrinsic scattering mechanisms.

[S0163-1829(99)05611-8]

I. INTRODUCTION

Modern growth techniques such as liquid phase epitaxy or molecular beam epitaxy have made possible the fabrication of semiconductor superlattices (SLs) that have optical, electrical, and vibrational properties not found in bulk semiconductors. Extensive studies have been performed on both the fundamental properties and practical applications of these systems.^{1,2} Experimental and theoretical studies of vibrational properties have primarily concentrated on the SL phonon dispersion.³ Superlattice interfaces have also been investigated in detail using vibrational spectroscopy.³ Because the phonon dispersion relation is substantially modified in a SL, it is reasonable to expect that the thermal transport properties of a SL will differ substantially from those of its bulk constituents.

The thermal conductivity of semiconductors is limited by the rate at which phonons are scattered. Phonon scattering processes can be divided into *intrinsic* processes, arising from the anharmonicity of the interatomic forces, and *extrinsic* processes due to phonon scattering at various sorts of crystal defects and at the crystal surface. Peierls⁴ pointed out that the anharmonic processes were of two distinct types. For normal (N) processes the vector sum of the phonon momenta is unchanged after a collision, whereas for umklapp (U) processes the total momentum changes by a reciprocal-lattice vector. In a bulk crystal, there is a minimum phonon energy required for a U process to occur. In a SL, this energy is reduced relative to the bulk because the magnitude of the shortest reciprocal-lattice vectors is smaller. Furthermore, the minimum energy for umklapp processes can be tuned by

varying the repeat distance. Therefore, measurements of the temperature dependence of the thermal conductivity of a family of high-quality SLs can be used to study umklapp scattering processes.

On a practical level, a more complete understanding of the processes that govern the flow of heat through SLs is of importance for the design of quantum-well lasers^{5,1} and SL thermoelectric devices.^{6,7} For a quantum-well laser it is advantageous to use a SL structure that has as high a thermal conductivity as possible, whereas for thermoelectric cooling and power conversion low thermal conductivity is required.

In a SL structure it is necessary to distinguish between the thermal conductivity perpendicular κ_{\perp} or parallel κ_{\parallel} to the SL interfaces. It was predicted over 15 years ago that κ_{\perp} of SLs should be reduced compared to the weighted average of the bulk constituents.⁸ Since that time, there have been only a few measurements of SL thermal conductivity. This is due to a large extent to the difficulty of measuring the heat flow in very small structures.

Most of the measurements of the thermal conductivity of SLs have been made by using an ac calorimetric apparatus.⁹ In the first of these experiments, κ_{\parallel} of several $(\text{GaAs})_n/(\text{AlAs})_n$ SLs was measured at 300 K.¹⁰ The thickness of each layer ranged from about $n=17$ to 177 monolayers (ML). It was found that κ_{\parallel} of the SLs was smaller than the average conductivity of the bulk constituents. There was a decrease in κ_{\parallel} with a decrease in the SL period, and the conductivity for the shortest period SLs was close to that of the $\text{Al}_{0.5}\text{Ga}_{0.5}\text{As}$ alloy. This technique was later used to measure the thermal diffusivity at 300 K in the directions parallel and perpendicular to the surface of a vertical-cavity

surface emitting laser (VCSEL) made from layers of GaAs and $\text{Al}_x\text{Ga}_{1-x}\text{As}$.¹¹ Due to the complicated structure, a thermal diffusivity value was not assigned to a particular SL but rather to the whole VCSEL structure. A substantial decrease of the thermal diffusivity compared to the bulk constituents was found for both directions; the decrease in κ_{\perp} was slightly larger than the decrease in κ_{\parallel} . More recently, the ac calorimetric method was used to measure the temperature dependence of κ_{\parallel} in a $(\text{GaAs})_n/(\text{AlAs})_n$ SL with $n \approx 247$.^{12,13} The measurements were made over a temperature range of 190–450 K. The SL had κ_{\parallel} slightly lower than GaAs throughout most of the temperature range, with the largest difference being $\sim 10\%$ at 190 K.

The thermal conductivity of SLs has been measured with two other techniques. We have previously reported some preliminary measurements of κ_{\perp} of two short-period $(\text{GaAs})_n/(\text{AlAs})_n$ SLs.^{14,15} Approximately an order of magnitude decrease in κ_{\perp} compared to GaAs was found for both a $(\text{GaAs})_3/(\text{AlAs})_3$ and a $(\text{GaAs})_{12}/(\text{AlAs})_{14}$ SL over the temperature range of 80–330 K. More recently, the 3ω method¹⁶ was used to measure the thermal conductivity of Si_m/Ge_n SLs over the temperature range 80–400 K.¹⁷ The samples had Si or Ge layers with different thickness, ranging from 5 to 146 ML. There was over an order of magnitude decrease in the thermal conductivity of the Si_m/Ge_n SLs compared to the average of the conductivity of the bulk constituents at the high temperatures. At low temperatures the decrease was even larger.

In this paper we describe how the optical pump-and-probe technique can be used to determine $\kappa_{\perp}(T)$ of a thin layer, and present the results of measurements of $\kappa_{\perp}(T)$ for a family of $(\text{GaAs})_n/(\text{AlAs})_n$ SLs.

II. EXPERIMENT

A. Transient heat-flow techniques

The experimental determination of the thermal conductivity of a material can be made either by a steady-state or a time-dependent heat flow method.¹⁸ In a steady-state experiment, heat is supplied at one point of a sample and extracted at another point by a heat sink. It is difficult to use this approach to determine the thermal conductivity of a thin layer on a substrate. If, for example, the heat flow is between two points on the free surface of the layer, the distance between these points must be much less than the layer thickness so that the substrate does not influence the heat flow. A measurement of the heat flow in a free-standing plate avoids the problem of substrate conduction, but sample preparation is then more difficult. In addition, in the steady-state technique it is necessary to have several contacts to the sample in order to supply the heat, extract it, and measure the relevant temperature difference. To overcome these difficulties, a time-dependent method can be used. Most of the techniques of this type require at most a single contact to be made to the surface of the sample. Very thin structures, either free standing or on a substrate, can be measured with these techniques.

Hatta *et al.*⁹ have used an ac calorimetric method to measure the thermal diffusivity D_{\parallel} in the direction parallel to the surface of a free-standing thin plate. In this technique, the sample surface is partly covered by a mask, and the uncovered portion is irradiated by light chopped at frequency f .

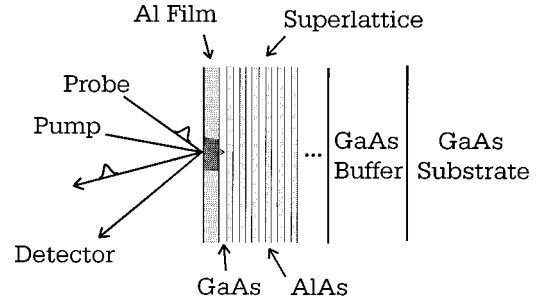


FIG. 1. Schematic diagram of the experiment and sample structure

The frequency is chosen in order to satisfy the condition $\pi f d^2/D_{\parallel} \ll 1$, where d is the thickness of the sample. Under this condition, the temperature is uniform throughout the thickness of the sample, and the temperature wave propagates in the plane parallel to the sample surface. If the heat capacity C of the material is known, κ_{\parallel} can be calculated by using the relation $\kappa_{\parallel} = CD_{\parallel}$. Several groups have used this technique to measure D_{\parallel} of SLs.^{10–12}

The 3ω method developed by Cahill¹⁶ has been applied to the measurement of the thermal conductivity of Si_m/Ge_n SLs.¹⁹ This technique is closely related to previously developed hot-wire²⁰ and hot-strip²¹ techniques. The method uses a single metallic film in the form of a strip running across the sample surface to both generate heat and detect the surface temperature. In the experiment, an ac current with frequency ω is passed through the metal strip. This gives a heat source of frequency 2ω . The temperature oscillations of the strip cause the resistance of the metal to have an oscillatory component at 2ω . This resistance oscillation causes a 3ω component of the voltage across the line. The thermal conductivity is determined by analyzing the magnitude of the 3ω component as a function of ω . The technique probes the sample to a depth of the order of

$$\xi = \left(\frac{D_{\perp}}{2\omega} \right)^{1/2}, \quad (1)$$

where D_{\perp} is the thermal diffusivity perpendicular to the sample surface. If the strip is wide compared to the penetration depth ξ , then the temperature at any point in the sample depends only on the distance z from the surface, and so a one-dimensional analysis can be used to calculate κ_{\perp} . Measurements on Si_m/Ge_n SLs were performed over a wide frequency range, but typically data were obtained for a frequency near 1 kHz. In these experiments, the penetration depth of the temperature wave was larger than the thickness of the Si_m/Ge_n SLs, and heat flow into the underlying material had to be taken into account.

B. Pump-and-probe technique

In the experiments reported here we have used an optical pump-and-probe technique. This technique has the advantage of a much shorter effective penetration depth, and therefore is well suited for measurements on a very thin layer, such as a SL. In the experiment, a metallic film, usually aluminum, is deposited on the sample layer (Fig. 1). A pump light pulse,

focused to a small spot on the surface of the metallic film, creates a sudden temperature rise. A small change in the temperature of the film $\Delta T(t)$ produces a proportional change in the optical reflectivity $\Delta R(t)$. The change in the reflectivity as the film cools by conduction into the underlying structure is measured by means of a time-delayed probe light pulse which is focused onto the film so as to overlap with the pump pulse. In order to determine κ_{\perp} , the change in the reflectivity as a function of delay time is compared to a change calculated from a numerical simulation of the heat flow. The value of κ_{\perp} used in the simulation is adjusted so as to give the best fit to the experimental data. The Al film cools in a few ns, and in this time the heat penetrates only a few hundred nm into the sample. Hence, even for samples as thin as $1 \mu\text{m}$, the effect of heat flow into the substrate is very small. This technique has previously been used to measure the thermal conductivity of amorphous diamond films,²² semiconductor SLs,¹⁴ and isotopically enriched Si.²³

To determine the thermal conductivity, it is necessary to make an accurate measurement of the reflectivity change $\Delta R(t)$ for a time delay of the probe varying from about 100 ps to several ns. In order to make a measurement of this type, it is necessary to maintain a constant overlap of the pump-and-probe beams on the metallic film while the probe time delay is varied. An optical system capable of this type of measurement has been described in Ref. 15, and a similar system was used here. In this apparatus the light pulses are produced by a Ti:sapphire laser operating at a repetition rate of 76 MHz, a wavelength of 800 nm, and a pulse duration of 250 fs. The pump beam is chopped at a frequency f of 1 MHz by an acousto-optic modulator and focused to a spot of diameter $\sim 20 \mu\text{m}$. The probe beam is focused to a spot of diameter $\sim 20 \mu\text{m}$ on the same region of the sample illuminated by the pump. The optical path length of the probe pulse is varied relative to the optical path length of the pump pulse by reflecting the beam off a retroreflector mounted on a mechanical translation stage. The energies in each pump-and-probe pulse applied to the film are typically 1.3 nJ and 0.02 nJ, respectively. To improve the signal-to-noise ratio, the output of the photodiode which detects the reflected probe beam is amplified by a lock-in amplifier which has as its reference source the same 1 MHz signal that is used to drive the acousto-optic modulator.

When the pump light is absorbed, electrons near the front surface of the Al film are excited to higher energy states. These hot electrons quickly diffuse away from the Al surface, but are confined to the Al film by the Schottky barrier at the Al-SL interface. Within several picoseconds, the hot electrons transfer their excess energy to the lattice by electron-phonon collisions, slightly raising the temperature of the Al film.²⁴ The temperature distribution inside the Al film becomes uniform by thermal diffusion, and phonons escape across the interface into the SL. The diffusion of the phonons across the interface is a relatively slow process compared to the thermal transport within the Al film. Therefore, the time constant τ for the temperature to become uniform inside the film can be approximated by the time constant for the same process in an insulated Al film, i.e.,

$$\tau \approx \frac{d_{\text{Al}}^2}{\pi^2 D_{\text{Al}}}, \quad (2)$$

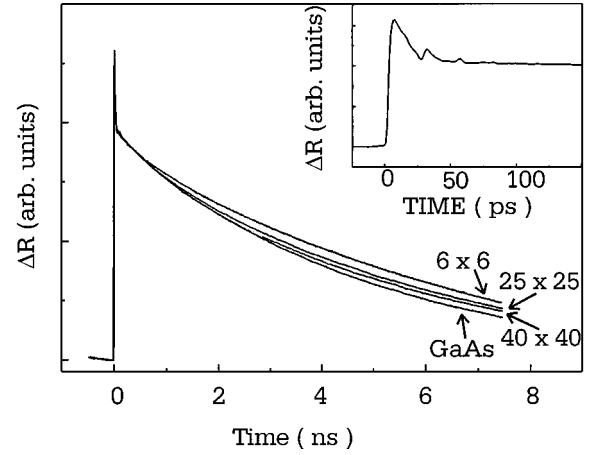


FIG. 2. Measured change $\Delta R(t)$ in optical reflectivity as a function of time after application of the heating light pulse. These data are for bulk GaAs and for $n \times n$ GaAs/AlAs superlattices with $n = 6, 25$, and 40 . The inset shows data taken on the GaAs sample for shorter times. The sharp features in the inset arise from acoustic echoes in the Al film.

where d_{Al} is the thickness of the film and D_{Al} is the thermal diffusivity of Al. For an Al film that is 100 nm thick with diffusivity of $0.45 \text{ cm}^2 \text{ s}^{-1}$,²⁵ τ is 23 ps at 300 K. The increase in the temperature of the film from a single pump pulse is

$$\Delta T = \frac{(1-R)Q}{C_{\text{Al}} A d_{\text{Al}}}, \quad (3)$$

where R is the optical reflectivity of the film ($\sim 90\%$ for Al), Q is the energy of the pump pulse, C_{Al} is the specific heat per unit volume of Al, and A is the area of the spot. For a pump pulse with an energy of 1.3 nJ and an Al thickness of 100 nm, the increase in the temperature of the Al film is about 2 K at room temperature.

As already described, a measurement of the change in the reflectivity versus time delay, $\Delta R(t)$, can be used to give the rate at which the Al film cools. Four cooling curves obtained at 300 K are displayed in Fig. 2. The labels at the end of each curve refer to the structure immediately below the Al film. In order to compare the cooling curves, the measured $\Delta R(t)$ from each sample have been scaled so that the curves overlap for time delays just before and just after $t=0$. The Al thickness on top of each sample was approximately 87 nm. The inset shows the details of the first 150 ps of the change in the reflectivity for the $(\text{GaAs})_{25}/(\text{AlAs})_{25}$ SL. The decrease in $\Delta R(t)$ which occurs within the first 40 ps is mainly due to the redistribution of the heat within the Al film. The slower decrease of $\Delta R(t)$ at later times is due to the cooling of the film into the underlying structure. One can see from Fig. 2 that the Al film cools fastest on the GaAs substrate and the cooling rate of the SLs increases with decreasing SL period.

The sharp features that can be seen in the inset of Fig. 2 are acoustic echos. When the light is absorbed, the temperature rise sets up an inhomogeneous stress distribution, which on relaxing launches a strain pulse from the surface of the film. The pulse propagates back and forth in the Al film, decreasing in amplitude after each reflection at the Al-SL interface. Each time the pulse returns to the free surface of

the Al film, the elastic strain alters the optical properties of the film near the surface causing a small change in the optical reflectivity. The time interval between these features is used to calculate the thickness of the film.²⁶

The analysis of the cooling of the Al film into the sample is greatly simplified because it is possible to ignore heat flow in the radial direction in the Al film and SL. Consider first the response $\Delta R(t)$ that would be obtained for an Al film which is thermally insulated on both sides. In such a sample the region heated by the pump pulse cools solely by radial heat diffusion. We take the intensity of the pump beam to vary laterally as $\exp(-r^2/r_0^2)$, where r is the distance from the center of the pump spot and r_0 is a constant. Then the initial temperature distribution in the Al film (assumed to be uniform throughout the thickness) will be

$$\Delta T(r, t=0) = \Delta T_0 \exp(-r^2/r_0^2). \quad (4)$$

At later times the temperature distribution will be²⁷

$$\Delta T(r, t) = \frac{\Delta T_0 r_0^2}{r_0^2 + 4D_{\text{Al}}t} \exp\left(-\frac{r^2}{r_0^2 + 4D_{\text{Al}}t}\right). \quad (5)$$

The change in the reflectivity of the probe pulse is proportional to the convolution of the temperature profile with the intensity profile of the probe. This intensity profile is approximately the same as the profile of the pump. It follows that

$$\Delta R(t) = \Delta R(0) \left/ \left(1 + \frac{2D_{\text{Al}}t}{r_0^2}\right)\right., \quad (6)$$

where $\Delta R(0)$ is the reflectivity change at $t=0$. We estimate that in the temperature range of our measurements D_{Al} lies between 0.45 and 0.62 $\text{cm}^2 \text{s}^{-1}$.²⁵ For $D_{\text{Al}} = 0.62 \text{ cm}^2 \text{ s}^{-1}$ and $r_0 = 10 \text{ }\mu\text{m}$, Eq. (6) gives

$$\Delta R(t) = \Delta R(0) \left/ (1 + 1.24 \times 10^{-3}t)\right., \quad (7)$$

where t is in ns. Thus, within the time range of our measurements ($t \leq 7.5$ ns) the effect of radial heat flow for an Al film which is insulated on both sides is very small. Since the thermal diffusivity of the SL samples is less than that of the Al film, the effect of radial heat flow in the SL is also unimportant. Thus, in the analysis of our experiment it is a good approximation to assume that the heat flow is solely in the direction z normal to the sample surface.

Cooling of the Al film after the application of a single pump pulse can then be calculated as follows. For simplicity, we ignore the variation in intensity of the pump pulse across the sample surface, and consider that there is uniform illumination of an area A . Let the temperature of the Al film at time t be T_{Al} , and let $T_{\text{SL}}(z, t)$ be the temperature on the plane z in the SL. The top surface of the SL is at $z=0$. The rate \dot{Q} at which energy is transferred across the Al-SL interface is proportional to the temperature jump across the interface between the film and the SL, and is given by

$$\dot{Q} = \sigma_K A [T_{\text{Al}}(t) - T_{\text{SL}}(z=0, t)], \quad (8)$$

where σ_K is the Kapitza conductance. Thus, the rate of change of the temperature of the film is given by

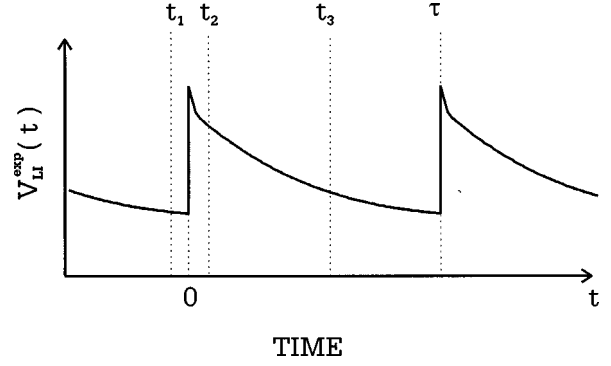


FIG. 3. Qualitative form of the in-phase lock-in output as a function of the time-delay t between the pump and probe. The times t_1 , t_2 , and t_3 are discussed in the text.

$$C_{\text{Al}} d_{\text{Al}} \frac{\partial T_{\text{Al}}(t)}{\partial t} = -\sigma_K [T_{\text{Al}}(t) - T_{\text{SL}}(z=0, t)]. \quad (9)$$

The heat flow within the SL is governed by the one-dimensional diffusion equation,

$$C_{\text{SL}} \frac{\partial T_{\text{SL}}(z, t)}{\partial t} = \kappa_{\perp} \frac{\partial^2 T_{\text{SL}}(z, t)}{\partial z^2}, \quad (10)$$

where C_{SL} is the heat capacity of the SL. For an assumed initial temperature rise of the aluminum film, Eqs. (9) and (10) can be solved numerically to predict the temperature of the film at later times, and hence the change in temperature $\Delta T_1(t)$ due to a single pump pulse.

The response to a single pump pulse does not fall to a negligible value by the time the next pump pulse arrives. It is therefore necessary to consider in the analysis the contributions to $\Delta T(t)$ and $\Delta R(t)$ that come from previous pump pulses. The response of the detection system when $\Delta R(t)$ originates from more than one pump pulse was discussed in Ref. 15. It was shown that the in-phase part of the lock-in signal V_{LI} , i.e., the output when the lock-in reference is in phase with the modulation of the pump light pulses, is approximated by (Eq. 12 of [15])

$$\begin{aligned} V_{\text{LI}}(t) &= \frac{\alpha}{\tau} \sum_{q=-\infty}^{\infty} \cos[2\pi f(q\tau + t)] \Delta R_1(q\tau + t) \\ &= \frac{\alpha\beta}{\tau} \sum_{q=-\infty}^{\infty} \cos[2\pi f(q\tau + t)] \Delta T_1(q\tau + t). \end{aligned} \quad (11)$$

In this equation, α is a constant, β is the thermoreflectance coefficient [$\Delta R_1(t) = \beta \Delta T_1(t)$], f is the modulation frequency (1 MHz), τ is the spacing between pump pulses (≈ 13.16 ns), t is the time delay of the probe relative to the pump, and $\Delta R_1(t)$ is the change in reflectivity that would result at a time t after the application of a *single* pump pulse. For our measurement system, the value of α has not been determined, and we have not measured the thermoreflectance coefficient β for the Al films prepared in our laboratory. Equation (11) is valid provided that $2\pi f\tau$ is much less than unity, and τ is much less than the lock-in time constant. These conditions are well satisfied in our experiments. $V_{\text{LI}}(t)$ is a periodic function of t , with period τ , and its form is shown qualitatively in Fig. 3. The out-of-phase part of the

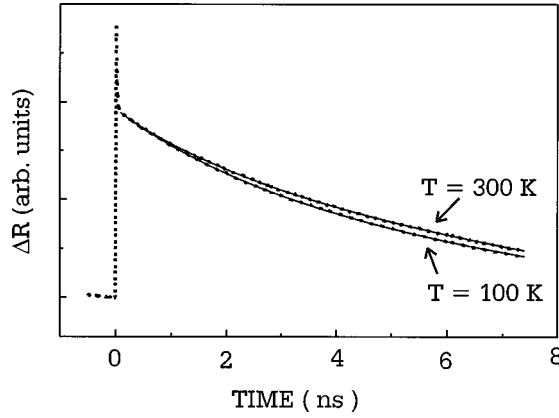


FIG. 4. Measured cooling curves of a 93 nm Al film on a (GaAs)₁₇/(AlAs)₁₇ superlattice at 100 and 300 K.

lock-in output is given by the same equation with $\cos[2\pi f(q\tau+t)]$ replaced by $\sin[2\pi f(q\tau+t)]$.

To determine the thermal conductivity κ_{\perp} from the measured lock-in output $V_{\text{LI}}^{\text{exp}}(t)$, the following procedure was used. The first step was to assume a value for the thermal conductivity κ_{\perp} and the Kapitza conductance σ_K . Equations (9) and (10) are then used to calculate the temperature $\Delta T_1(t)$ of the Al as a function of the time after application of a single pump pulse. In this calculation the bulk value of the heat capacity of Al is used for C_{Al} and the thickness of the film d_{Al} is determined by picosecond ultrasonics.²⁶ The heat capacity C_{SL} of the SL is taken to be a weighted average of the heat capacity of the constituents. In this average, the bulk value of the heat capacity of GaAs is used and the heat capacity of AlAs is calculated from a lattice-dynamical model.²⁸ From $\Delta T_1(t)$ a simulated lock-in output $V_{\text{LI}}^{\text{sim}}(t)$ is calculated to within an uncertainty arising from the unknown factor $\alpha\beta$. We then form the two quantities

$$S^{\text{exp}}(t) \equiv V_{\text{LI}}^{\text{exp}}(t) - V_{\text{LI}}^{\text{exp}}(t_1) \quad (12)$$

and

$$S^{\text{sim}}(t) \equiv V_{\text{LI}}^{\text{sim}}(t) - V_{\text{LI}}^{\text{sim}}(t_1), \quad (13)$$

where the time t_1 corresponds to the probe pulse arriving slightly before the pump (see Fig. 3). We then adjust $\alpha\beta$ so as to minimize the quantity

$$\Sigma = \int_{t_2}^{t_3} dt [S^{\text{exp}}(t) - S^{\text{sim}}(t)]^2. \quad (14)$$

The integration over time is from t_2 (75 ps) to t_3 (7.5 ns) (see Fig. 3). The time t_2 is chosen to be just after the temperature distribution throughout the thickness of the Al film has become uniform, and the time t_3 is the end point of the measured data. This entire procedure is then repeated with different values of κ_{\perp} and σ_K until the minimum of Σ is found. The fits to $V_{\text{LI}}^{\text{exp}}(t)$ of 93 nm of Al on a (GaAs)₁₇/(AlAs)₁₇ SL measured at 100 and 300 K are displayed in Fig. 4. To reduce the error in the measurement of κ_{\perp} , up to eight cooling curves were often taken on a single sample at a given temperature and the fit parameters averaged to obtain a single κ_{\perp} value. The final uncertainty in the measured κ_{\perp} was typically $\pm 10\%$.

In the above analysis we have ignored heat flow into the GaAs below the SL. In order to account for heat flow into the material below the SL, the procedure that is used to determine $\Delta T_1(t)$ must be modified to include the diffusion of heat across the interface between the SL and the GaAs, and through the GaAs. We take the thermal conductivity and heat capacity of the GaAs to be the same as in bulk. We investigated the effect of a Kapitza resistance between the SL and the GaAs, and found that, for any reasonable value, the effect on the cooling rate of the Al film was unimportant. Thus, the only significant parameters continue to be the Kapitza conductance σ_K at the Al-SL interface and the thermal conductivity κ_{\perp} of the SL. It was found that heat flow into the GaAs was important only for the (GaAs)₂₅/(AlAs)₂₅ and (GaAs)₄₀/(AlAs)₄₀ SLs at temperatures ≤ 150 K.

One can think of alternative methods for the determination of κ_{\perp} and σ_K from $V_{\text{LI}}(t)$. For example, one could use the out-of-phase lock-in output over some time range, as well as the in-phase output. However, the out-of-phase signal will be more sensitive to errors associated with radial heat flow, and thus a correction for this effect would probably have to be applied.

As a test of the technique we have made room-temperature measurements of the thermal conductivity of Al₂O₃, GaAs, Ge, Si, and amorphous SiO₂ samples, and have obtained results within 10% of the accepted values. The thermal conductivity of these materials varies from 0.014 to 1.48 W cm⁻¹K⁻¹. The technique cannot be applied to measure κ for materials of very high thermal conductivity, such as diamond, because the cooling of the Al film is then almost entirely limited by the Kapitza conductance, rather than by the thermal conductivity of the sample.²⁹ For very low thermal conductivity materials, the steady-state heating of the sample surface by the pump-and-probe pulses is a significant limiting factor.

The thermal conductivity $\kappa_{\perp}(T)$ of the (GaAs)_{*n*}/(AlAs)_{*n*} SLs was measured over the temperature range 100–375 K by using a liquid N₂ flow cryostat. At low temperatures, the heating of the Al film due to a pump pulse of sufficient energy to be detected by the probe pulse is no longer small compared to the substrate temperature. For this reason, we are limited to taking measurements at or above 100 K. The high-temperature limit of the experiment, 375 K, was set by the performance of the heater in the cryostat.

C. Samples

The SLs were grown by molecular beam epitaxy at the Max-Planck-Institut für Festkörperforschung (MPI) and at the Naval Research Laboratory (NRL). Sample properties are listed in Table I. Most of the samples were grown on a GaAs buffer layer of at least 200 nm thickness which was deposited on a (001) GaAs substrate. Two of the samples were grown directly on a GaAs substrate. The layer thickness of the $n=6$, 10, and 17 SLs was confirmed by x-ray diffraction. For all samples, the final SL layer was always GaAs.

A number of postgrowth characterization techniques can be used to assess the interface quality of semiconductor SLs.^{30,31} It is commonly accepted that the transition region at interfaces in high-quality (GaAs)_{*m*}/(AlAs)_{*n*} SLs is 1–2 ML thick and consists of large atomically flat terraces with small-

TABLE I. Structural and growth parameters of the superlattices used. The number of superlattice periods is l , and n denotes the number of monolayers in each layer. The total thickness of the superlattice is d_{SL} . The superlattices were grown on a buffer layer of thickness d_{buffer} at a substrate temperature of T_{sub} and with a growth interrupt time t_{int} . The thickness of the Al film is d_{Al} .

Grower	n	l	d_{SL} (nm)	T_{sub} ($^{\circ}\text{C}$)	d_{buffer} (nm)	t_{int} (s)	d_{Al} (nm)
MPI	1	800	452.8	550	200	8	99
MPI	2	400	452.8	495	200	9	99
NRL	3	159	270.0	590	500	unknown	94
MPI	6	150	509.4	530	0	20	87
MPI	10	150	849.0	555	0	20	91
NRL	17	50	481.1	800	500	90	93
NRL	25	15	212.3	580	450	90	87
NRL	40	10	226.4	580	450	90	87

scale microroughness.^{32–36} The lateral size of the islands depends on the conditions during the growth process. The largest terraces (>25 nm) are formed when AlAs is deposited on GaAs. For GaAs deposited on AlAs, the terraces may be as small as 4–6 nm. The sharpest interfaces are obtained by growing a buffer layer to isolate the SL from the surface imperfections of the GaAs substrate,³⁷ and by using growth interrupt in order to allow for the recovery of the surface smoothness before the next layer is deposited.^{38,39}

Photoluminescence (PL) measurements can be used to partially characterize the roughness of an interface. The energy of the PL peak depends on the average thickness of the GaAs well, and the width of the peak or the presence of additional peaks indicates long-range monolayer fluctuations or interfacial microroughness, respectively.³¹ Photoluminescence measurements were made on the SLs grown at MPI ($n=1,2,6,10$). It was found that the PL energies of the Γ - Γ and Γ - X excitons agree reasonably well with those expected for ideal structures. The broadening of the PL peaks was less than the energy corresponding to a layer thickness fluctuation of 1 ML. This is indicative of rather smooth interfaces on the length scale of the exciton diffusion length (≈ 25 nm³¹), which, however, could still have microroughness.

An Al film was deposited on each SL sample by thermal evaporation. The pressure during the Al deposition was typically 5×10^{-6} torr. It is essential that the reflectivity changes $\Delta R(t)$ arise solely from the change in temperature of the Al. Thus, the Al film must have a minimum thickness in order to prevent light from reaching the SL sample. However, in order to minimize the temperature gradient in the Al film, the film thickness should be as close to this minimum value as possible. The optical absorption length of a thin metallic layer depends on the deposition conditions during the growth of the film.⁴⁰ In order to give sufficient absorption of the laser light, we found it necessary to use films with a thickness of at least 80 nm in order to give sufficient absorption of the laser light. The dependence of the measured thermal conductivity of GaAs at 300 K for samples with different Al thickness is shown in Fig. 5. The accepted value of κ_{GaAs} at 300 K is $0.46 \text{ W cm}^{-1} \text{ K}^{-1}$. The dashed lines correspond to a range of $\pm 5\%$ around this value. For samples that have an Al thickness within the range of about 80–120 nm, the measured thermal conductivity agrees with this accepted value.

The thickness of each Al film on the SL samples we studied was measured by picosecond ultrasonics and was found to be between 87 and 99 nm.

III. RESULTS AND DISCUSSION

The temperature dependence of the thermal conductivity $\kappa_{\perp}(T)$ for the $(\text{GaAs})_n/(\text{AlAs})_n$ SLs is displayed in Fig. 6. We find a general increase in κ_{\perp} with an increase of the SL period. At 300 K, κ_{\perp} of the $(\text{GaAs})_{40}/(\text{AlAs})_{40}$ SL is approximately three times less than κ of bulk GaAs, whereas κ_{\perp} of the $(\text{GaAs})_1/(\text{AlAs})_1$ SL is an order of magnitude less than κ of bulk GaAs. As the temperature is decreased, κ_{\perp} of the SLs increases. At 100 K, κ_{\perp} of the $(\text{GaAs})_{40}/(\text{AlAs})_{40}$ SL is approximately 10 times less than κ of bulk GaAs, and κ_{\perp} of the $(\text{GaAs})_1/(\text{AlAs})_1$ SL is approximately 20 times less than κ of bulk GaAs. It is remarkable that the conductivity of the short-period superlattices is *less* than the conductivity of the $\text{Al}_{0.5}\text{Ga}_{0.5}\text{As}$ alloy ($\kappa = 0.12 \text{ W cm}^{-1} \text{ K}^{-1}$).²

The results show that, in general, κ_{\perp} decreases monotonically as the SL period is decreased, although there are some

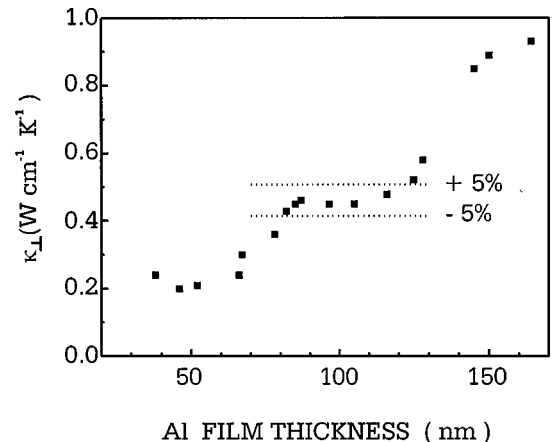


FIG. 5. Results of a series of measurements of the thermal conductivity of bulk GaAs using Al films of different thickness d_{Al} . For d_{Al} between 80 and 120 nm the measured conductivity is independent of d_{Al} .

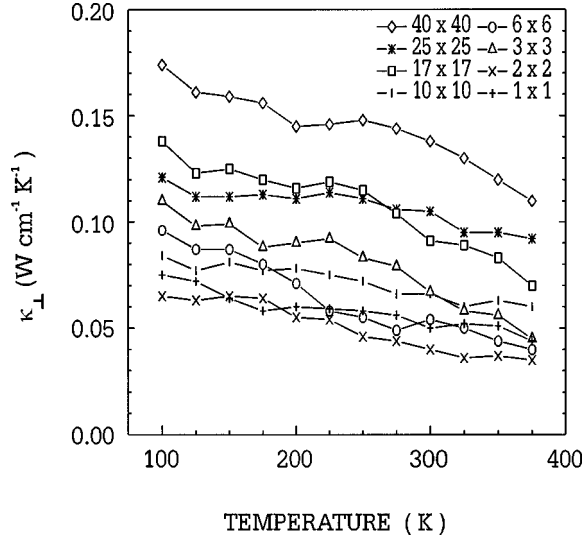


FIG. 6. The temperature dependence of the thermal conductivity κ_{\perp} perpendicular to the superlattice interfaces for $n \times n$ GaAs/AlAs superlattices, where n is the number of monolayers in each superlattice layer.

deviations from this trend (see Fig. 6), which are significantly larger than the error in the measurements. A more complex behavior was found by Lee *et al.* for Si_m/Ge_n .¹⁷ At 200 K, two SLs with periods of 3 and 3.3 nm were found to have $\kappa_{\perp} \sim 0.03 \text{ W cm}^{-1} \text{ K}^{-1}$, whereas three SLs with periods between 5 and 6.5 nm had $\kappa_{\perp} \sim 0.04 \text{ W cm}^{-1} \text{ K}^{-1}$. Thus, for these samples κ_{\perp} decreases with decreasing SL period, as we have found. However, for three samples with SL period greater than 13 nm, the value of κ_{\perp} was considerably lower. This decrease was attributed to the presence of a high density of dislocations and stacking faults in these large-period samples. However, for GaAs/AlAs the lattice mismatch is very small, and so an increase in defect concentration for large-period SLs is unlikely to occur.

Lee *et al.*¹⁷ found that for all of their Si_m/Ge_n SLs, κ_{\perp} increased with increasing temperature over the temperature range 80–200 K, and was approximately constant between 200 and 400 K. This contrasts with the steady decrease in conductivity that we observe for $(\text{GaAs})_n/(\text{AlAs})_n$ between 100 and 375 K.

At present there is no satisfactory quantitative theory of the thermal conductivity in SLs which can account for its dependence on both period and temperature.^{41,42} The ratio of the temperature-dependent phonon mean free path Λ in the constituent bulk materials to the SL period d_{SL} is clearly a significant parameter. Consider first a SL that has perfectly smooth interfaces, and no defects or impurities. Let the thickness of the layers of the two components 1 and 2 making up the SL be d_1 and d_2 , and let the thermal conductivity of the bulk constituents be κ_1 and κ_2 , respectively. One can distinguish three regimes.

(A) If $d_{\text{SL}} \gg \Lambda$, the thermal resistance of the SL will just be the weighted average of the bulk thermal resistivities. Thus,

$$\frac{1}{\kappa_{\perp}} = \frac{1}{d_1 + d_2} \left(\frac{d_1}{\kappa_1} + \frac{d_2}{\kappa_2} \right). \quad (15)$$

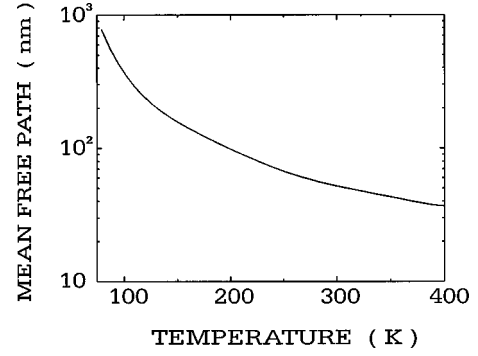


FIG. 7. The temperature dependence of the mean free path Λ of thermal phonons in GaAs. The mean free path was calculated using the equation $\Lambda = 3 \kappa / C \langle v \rangle$, where κ is the thermal conductivity of bulk GaAs, C is the heat capacity of GaAs, and $\langle v \rangle$ is the average thermal phonon velocity in GaAs.

(B) If $d_{\text{SL}} \sim \Lambda$, the result just given should be corrected for the Kapitza resistance at each interface. Thus,

$$\frac{1}{\kappa_{\perp}} = \frac{1}{d_1 + d_2} \left(\frac{d_1}{\kappa_1} + \frac{d_2}{\kappa_2} + \frac{2}{\sigma_K} \right), \quad (16)$$

where σ_K is the Kapitza conductance of the GaAs/AlAs interface.

(C) If $d_{\text{SL}} \ll \Lambda$, a phonon will be reflected or transmitted at many interfaces before it is scattered *within* a layer of the SL. Under these conditions it makes sense to consider that the effect of the SL is to modify the phonon-dispersion relation. New gaps appear in the dispersion relation when the magnitude of the component of the phonon wave vector normal to the SL planes equals integer multiples of π/d_{SL} . If a reduced zone scheme is used, these new gaps are at the boundary and the center of the new Brillouin zone. Of course, in addition to the appearance of these gaps, the dispersion relation is also modified (to some extent) throughout the zone, e.g., at internal gaps.^{3,43}

One can estimate the average phonon mean free path in a bulk material from the thermal conductivity through the use of the kinetic formula

$$\Lambda = \frac{3 \kappa}{C \langle v \rangle}, \quad (17)$$

where C is the specific heat per unit volume and $\langle v \rangle$ is the average phonon velocity. The Debye velocity v_D can be used for $\langle v \rangle$, but it has been shown⁴⁴ that when this is done this formula *underestimates* the value of Λ by a correction factor which is about 2.5 for temperatures above one-third of the Debye temperature Θ_D . The results for Λ in GaAs, including this correction factor, are as shown in Fig. 7. The mean free path decreases with increasing temperature but even at 375 K its value (40 nm) is more than twice the period d_{SL} for all the SLs that we have studied. Thus, our measurements are made in regime C.

Given this result, the thermal conductivity of the SL can be written as

$$\kappa_{\perp} = \frac{1}{3} C \langle v_{\perp}^2 \rangle \tau, \quad (18)$$

where v_{\perp} is the group velocity in the direction perpendicular to the layers calculated from the phonon-dispersion relation for the SL, and τ is the phonon scattering time. In a recent interesting paper, Hyldgaard and Mahan⁴⁵ have considered a simplified model of a Si_2/Ge_2 SL and have found that above 100 K the value of $\langle v_{\perp}^2 \rangle$ is reduced by a factor of about 10 compared to the average of the Si and Ge values. The reduction in v_{\perp} is particularly pronounced for phonons traveling at oblique incidence. As far as we know, a similar calculation has not yet been performed for the GaAs/AlAs system, and the details of how the reduction varies with repeat distance are not known. Nevertheless, the results of Hyldgaard and Mahan suggest that the reduction in $\langle v_{\perp}^2 \rangle$ may be large enough to explain the reduction in κ_{\perp} (see also 44).

It is also possible that a reduction in the phonon lifetime makes a significant contribution to the reduction in the conductivity. In a perfect bulk crystal the phonon lifetime entering Eq. (18) into the kinetic formula is determined by the combined effects of umklapp processes (U) and elastic scattering from isotopes. For temperatures below the Debye temperature the umklapp scattering rate decreases rapidly because high-energy phonons are required for a U process to occur. In a SL the energy required to produce a U process is reduced, and so at least for $T < \Theta_D$ the phonon lifetime will be less than in a bulk material. Ren and Dow⁸ have investigated this reduction within a simplified one-dimensional model. Even when the difference in the properties of the two layers is large (e.g., when the mass ratio is 2:1), the change in scattering time is modest (at most 25%). However, it is possible that the change may be much larger in a more detailed model which includes the change in lifetime for phonons traveling at oblique incidence.

At high temperatures such that $T \geq \Theta_D$ all phonon modes will have appreciable occupation. Thus, in this temperature range the average $\langle v_{\perp}^2 \rangle$ will be essentially independent of T . The umklapp scattering rate by three-phonon interactions will be proportional to T and, correspondingly, the thermal conductivity should vary as T^{-1} . At lower temperatures the conductivity of perfect crystals varies more rapidly with temperature.⁴ However, for the SLs we find a temperature dependence which is *slower* than T^{-1} (see Fig. 6). This temperature dependence also shows a significant variation from sample to sample (see Fig. 6). The differences presumably

result from phonon scattering at defects within the layers or at the interfaces. Chen⁴¹ has considered the limit of strong interface scattering, in which there is completely diffuse scattering at each SL interface. In this model the heat flow in each layer is governed by the bulk phonon dispersion, and the diffuse scattering causes a thermal boundary resistance at every SL interface. If the scattering is dominated by elastic scattering processes, the lifetime of each phonon will be a function of the phonon wave vector and polarization, but will be independent of the temperature. It then follows that the thermal conductivity must be an *increasing* function of temperature, in contrast to what we have found. Thus, it appears that a more general model taking account of *some* degree of interface scattering is needed. Chen has recently generalized this calculation to include partly specular reflection at the interfaces while keeping the ballistic nature of the bulk transport.⁴² This generalization, while introducing the ratio of specular to diffuse scattering as an additional parameter, is still not able to account for the decrease of κ_{\perp} with increasing temperature shown in Fig. 6.

Since bulk scattering processes (phonon-phonon interactions) decrease with decreasing temperature, while defect scattering is typically temperature-independent in the temperature range investigated here, it is expected that the importance of defects will increase at low T . The data provide some evidence in support of this view. At the highest temperature (375 K), κ_{\perp} decreases in sequence for the samples with $n = 40, 25, 17,$ and 10 , whereas the results for smaller n are closely grouped. Thus, there is a systematic variation of κ_{\perp} with n , suggesting that defects do not play an important role. At 100 K, on the other hand, κ_{\perp} does not vary monotonically with n , even for the $n = 50, 25, 17,$ and 10 samples. In future work, we plan to investigate a series of thicker SL to study the crossover to region *B*, discussed above.

ACKNOWLEDGMENTS

We thank S. Tamura and P. Hyldgaard for helpful discussions and E. Gmelin for a critical reading of the manuscript. This work was supported at Brown University by the U.S. Department of Energy under Grant No. DE-FG02-86ER45267.

¹C. Weisbuch and B. Vinter, *Quantum Semiconductor Structures* (Academic Press, San Diego, CA, 1991).

²S. Adachi, *GaAs and Related Materials* (World Scientific Publishing, Singapore, 1994).

³B. Jusserand and M. Cardona, in *Light Scattering in Solids V—Superlattices and Other Microstructures*, edited M. Cardona and G. Güntherodt (Springer-Verlag, Berlin, 1989), Chap. 3, p. 49.

⁴R. Peierls, *Ann. Phys. (Leipzig)* **3**, 1055 (1929).

⁵A. Yariv, *Quantum Electronics*, 3rd ed. (Wiley, New York, 1989).

⁶L. D. Hicks, T. C. Harman, and M. S. Dresselhaus, *Appl. Phys. Lett.* **63**, 3230 (1993).

⁷P. J. Lin-Chung and T. L. Reinecke, *Phys. Rev. B* **51**, 13 244 (1995).

⁸S. Y. Ren and J. D. Dow, *Phys. Rev. B* **25**, 3750 (1982).

⁹I. Hatta, Y. Sasuga, R. Kato, and A. Maesono, *Rev. Sci. Instrum.* **56**, 1643 (1985).

¹⁰T. Yao, *Appl. Phys. Lett.* **51**, 1798 (1987).

¹¹G. Chen, C. L. Tien, X. Wu, and J. S. Smith, *J. Heat Transfer* **116**, 325 (1994).

¹²X. Y. Yu, G. Chen, A. Verma, and J. S. Smith, *Appl. Phys. Lett.* **67**, 3554 (1995).

¹³X. Y. Yu, L. Zhang, and G. Chen, *Rev. Sci. Instrum.* **67**, 2312 (1996).

¹⁴W. S. Capinski and H. J. Maris, *Physica B* **219-220**, 699 (1996).

- ¹⁵W. S. Capinski and H. J. Maris, *Rev. Sci. Instrum.* **67**, 2720 (1996).
- ¹⁶D. G. Cahill, *Rev. Sci. Instrum.* **61**, 802 (1989).
- ¹⁷S. M. Lee, D. G. Cahill, and R. Venkatasubramanian, *Appl. Phys. Lett.* **70**, 2957 (1997).
- ¹⁸P. Brüesch, *Phonons: Theory and Experiments III* (Springer-Verlag, Berlin, 1987).
- ¹⁹D. G. Cahill, M. Katiyar, and J. R. Abelson, *Phys. Rev. B* **50**, 6077 (1994).
- ²⁰P. Andersson and G. Backström, *Rev. Sci. Instrum.* **47**, 205 (1976).
- ²¹S. E. Gustafsson and E. Karawacki, *Rev. Sci. Instrum.* **54**, 744 (1983).
- ²²C. J. Morath, H. J. Maris, J. J. Cuomo, D. L. Pappas, A. Grill, V. V. Patel, J. P. Doyle, and K. L. Saenger, *J. Appl. Phys.* **76**, 2636 (1994).
- ²³W. S. Capinski, H. J. Maris, E. Bauser, I. Silier, M. Asen-Palmer, T. Ruf, M. Cardona, and E. Gmelin, *Appl. Phys. Lett.* **71**, 2109 (1997).
- ²⁴G. Tas and H.J. Maris, *Phys. Rev. B* **49**, 15 046 (1994).
- ²⁵The value of D_{Al} was assumed to be the same as the diffusivity of Al films prepared in a similar way in our lab. The diffusivity was calculated by using the Wiedemann-Franz relation. The resistivity of Al was measured by a four-point probe technique. The diffusivity at 300 K was calculated to be $0.45 \text{ cm}^2 \text{ s}^{-1}$. In order to obtain the low temperature value ($0.62 \text{ cm}^2 \text{ s}^{-1}$ at 100 K) it was assumed that the decrease in the resistivity compared to bulk Al at 100 K would be the same as the change measured at 300 K. See Ref. 24.
- ²⁶H. T. Grahn, H. J. Maris, and J. Tauc, *IEEE J. Quantum Electron.* **25**, 2562 (1989).
- ²⁷K. Brugger, *J. Appl. Phys.* **43**, 577 (1972).
- ²⁸H. M. Kagaya and T. Soma, *Phys. Status Solidi B* **142**, 411 (1987).
- ²⁹R. J. Stoner and H. J. Maris, *Phys. Rev. B* **48**, 16 373 (1993).
- ³⁰*Optical Characterization of Epitaxial Semiconductor Layers*, edited by G. Bauer and W. Richter (Springer-Verlag, Berlin, 1996).
- ³¹M. A. Herman and H. Sitter, *Molecular Beam Epitaxy, Fundamentals and Current Status* (Springer-Verlag, Berlin, 1996).
- ³²M. Tanaka and H. Sakaki, *J. Cryst. Growth* **81**, 153 (1987).
- ³³M. A. Herman, D. Bimberg, and J. Christen, *J. Appl. Phys.* **70**, R1 (1991).
- ³⁴D. Gammon, B. V. Shanabrook, and D. S. Katzer, *Phys. Rev. Lett.* **67**, 1547 (1991).
- ³⁵B. Jusserand, F. Mollot, J. Moison, and G. Le Roux, *Appl. Phys. Lett.* **57**, 560 (1990).
- ³⁶T. Ruf, J. Spitzer, V. F. Sapega, V. I. Belitsky, M. Cardona, and K. Ploog, *Phys. Rev. B* **50**, 1792 (1994).
- ³⁷J. G. Pellegrino, S. B. Qadri, C. M. Cotell, P. M. Amirtharaj, N. V. Nguyen, and J. Comas, *J. Vac. Sci. Technol. A* **11**, 917 (1993).
- ³⁸A. R. Smith, K. Chao, C. K. Shih, Y. C. Shih, K. A. Anselm, and B. G. Streetman, *J. Vac. Sci. Technol. B* **13**, 1824 (1995).
- ³⁹H. Yu, P. B. Mookherjee, R. Murray, and A. Yoshinaga, *J. Appl. Phys.* **77**, 1217 (1995).
- ⁴⁰*Handbook of Thin Film Technology*, edited by L. I. Maissel and R. Glang (McGraw-Hill, New York, 1970), Chap 8.
- ⁴¹G. Chen, in *Micro-Electro-Mechanical Systems* (American Society of Mechanical Engineers, New York, 1996), Vol. 59, pp. 13–24.
- ⁴²G. Chen, *Phys. Rev. B* **57**, 14 958 (1998).
- ⁴³S. Tamura, D. C. Hurley, and J. P. Wolfe, *Phys. Rev. B* **38**, 1427 (1988).
- ⁴⁴R. J. Stoner and H. J. Maris, *Phys. Rev. B* **47**, 11 826 (1993).
- ⁴⁵P. Hyltdgaard and G. D. Mahan, *Phys. Rev. B* **56**, 10 754 (1997).